JOURNAL OF AIRCRAFT
Vol. 36, No. 5, September–October 1999

Validation Methods and Results for a Two-Dimensional Ice Accretion Code

William B. Wright*
DYNACS Engineering Company, Brook Park, Ohio 44142

A research project is underway at NASA Lewis Research Center (now called John H. Glenn Research Center at Lewis Field) to produce a library of computer codes that can accurately predict ice growth under any meteorological conditions for any aircraft surface. Results are presented from the most recent version of the two-dimensional code LEWICE. This version differs from previous releases due to its robustness and its ability to reproduce results accurately for different point spacing and time step criteria across several computing platforms. It also differs in the extensive amount of effort undertaken to compare the results in a quantifiable manner against the database of ice shapes that have been generated in the NASA Lewis Icing Research Tunnel. A quantitative method is described that has been applied to both the computational and experimental ice shapes. The result of this comparison shows that the difference between the predicted ice shape from LEWICE 2.0 and the average of the experimental data is 7.2% whereas the variability of the experimental data is 2.5%.

I. Introduction

THE icing branch at NASA Lewis Research Center (now called John H. Glenn Research Center at Lewis Field) has undertaken a research project to produce a computer code capable of accurately predicting ice growth under a wide range of meteorological conditions for any aircraft surface. The most recent release of this code is LEWICE 2.0. which will be documented in the new user manual.[1] This report will not go into the details of the capabilities of this code, as those features are well-described by the user manual.

The purpose of this paper is to present a summary of results from the complete set of data used for validation of LEWICE 2.0 as well as identify and assess criteria that are used to validate the NASA icing codes. Reference 2 provides more details of the cases studied. The criteria reviewed in this paper are not necessarily the only criteria that can be used for validation but they represent one possible path. The process for validation of an icing code is quite challenging and consists of many steps, one of which is the comparison of code results to some known solution, whether experimental or analytical. This testing activity is complicated because no predefined acceptance criteria have been identified. To date, previous evaluation of the performance of ice accretion prediction codes has been based on subjective judgements of the visual appearance of comparisons between ice shapes generated by the code and ice shapes measured in an experimental facility.[3–10]

To accurately determine the capabilities of a prediction code, it is necessary to develop quantitative measures for assessing the similarity between two ice shapes. The measurement used to make the comparison should be based on the characteristics considered most important for the purposes of the simulation process. For example, design of a thermal ice protection system may dictate that icing limits, accumulation rates, and total collection efficiency are the most important parameters to be simulated, whereas certification of a wing for flight with an ice accretion may require that the performance characteristics of the ice shape be modeled accurately.

In past reports,[11–16] LEWICE has been compared to shapes created in the NASA Lewis Icing Research Tunnel (IRT). Whereas many of these qualitative comparisons have been favorable, they do not demonstrate a validation process that quantitatively determines the accuracy of an ice accretion prediction code. Comparisons are made in this paper using a large subset of the data that have been generated in the IRT. The test entries that were not used for comparison represent ice shapes from proprietary tests or those tests for which the ice shapes were not digitized. The results are examined from a more quantitative approach than has been undertaken in previous efforts. Measured quantities are horn length, horn angle, stagnation point thickness, ice shape cross section, and icing limits. This paper will define the differences between experimental ice shapes and LEWICE 2.0, as well as the differences between two experimental ice shapes, where applicable.

Validation of an ice accretion prediction code can encompass more than just this comparison. The differences in aerodynamic performance for different shapes also needs to be quantified, both computationally and experimentally. Additionally, individual sections of the code, such as the droplet trajectory routine and the integral boundary-layer routine, can be validated as well.

The remainder of the paper is divided into four sections, plus a conclusions section. Section II provides a brief description of LEWICE and the LEWICE 2.0 model. Section III provides a description of the experimental data presented in this report. Section IV describes the quantitative parameters chosen and how they were measured. Section V presents results of the quantitative comparison. Comparison is made between measurements from ice shapes calculated using LEWICE 2.0 and the average measurements from the experimental data, as well as the comparison of individual experimental ice shapes against the same average. Spanwise variability and repeatability variability are presented, as well as the variability due to the technique used by the researcher to trace the ice shape.

II. LEWICE 2.0

The computer code LEWICE embodies an analytical ice accretion model that evaluates the thermodynamics of the freezing process that occurs when supercooled droplets impinge on a body. The atmospheric parameters of temperature and pressure, the meteorological parameters of liquid water content (LWC), droplet diameter, and relative humidity, and the flight parameters of velocity and angle of attack are specified and used to determine the shape of the ice accretion. The surface of the clean (uniced) geometry is defined by segments joining a set of discrete body coordinates. The code consists of four major modules. They are 1) the flow field calculation, 2) the particle trajectory and impingement calculation, 3) the thermodynamic and ice growth calculation, and 4) the modification of the current geometry by addition of the ice growth.

Received 26 October 1998; accepted for publication 29 January 1999.

*Research Engineer, Icing and Combustion Section, 2001 Aerospace Parkway. Senior Member AIAA.

LEWICE applies a time-stepping procedure to grow the ice accretion. Initially, the flowfield and droplet impingement characteristics are determined for the clean geometry. The ice growth rate on each segment defining the surface is then determined by applying the thermodynamic model. When a time increment is specified, this growth rate can be interpreted as an ice thickness, and the body coordinates are adjusted to account for the accreted ice. This procedure is repeated, beginning with the calculation of the flowfield about the iced geometry, then continued until the desired icing time has been reached.

LEWICE 2.0 is different from its predecessors not through wholesale changes in the physical models but rather through an extensive effort to adjust, test, and document the code to ensure: that the code runs correctly for all of the cases shown, that the quality of output is maintained across platforms and compilers, that the effects of time step and spacing have been minimized and demonstrated, that the code inputs and outputs are consistent and easy to understand, that the structure and documentation within the code makes it readily modifiable to those outside the standard LEWICE development team, and that the code has been validated in a quantified manner against the largest possible amount of experimental data. This last statement forms the basis of the comparisons in this report.

III. Description of the Experimental Data

The experimental data described in this paper are the result of a wide variety of tests performed in the IRT in recent years.[17–21] These tests included unpublished test entries by G. Addy in February 1998, D. Anderson in June 1996, S. Chen and T. Langhals in May 1998, G. Addy in February 1996, and C. S. Bidwell and J. F. VanZante in January 1998. Seven airfoils were selected for this comparison. The seven airfoils are a NACA 23014(modified), a large transport horizontal stabilizer (LTHS), a GLC 305 business jet airfoil, a NACA 0012, a NACA 0015, a NACA 4415(modified), and a Natural Luminar Flow (NLF) 0414. These airfoils and the accompanying ice shapes represent the complete set of publicly available data that has been generated in the IRT and digitized for single-element airfoils. There are some data available on multielement airfoils, but the data were considered an insufficient amount for validation purposes. There are a total of 395 IRT runs analyzed for this validation report, of which 164 are repeats of previous runs in the IRT. There are 440 digitized tracings at off-centerline locations and 7 duplicate tracings by a second researcher for a total of 842 experimental ice shapes. The duplicate tracings were taken to assess the impact of the tracing technique. Note that duplicate tracings were taken only when the researchers believed that differences would be found. Table 1 provides more details on the number of ice shapes for each airfoil.

The atmospheric, meteorological, and flight conditions covered by the experimental data encompass a wide range of values, as shown in Table 2. Table 2 specifies the range of conditions and airfoil sizes performed in the experimental tests. Note that the extremes of each range are not necessarily covered for all cases. This means that, although droplet distributions with a median volume diameter (MVD) up to 270 μm were run and LWC values up to 1.8 g/m^3 were run, the combination of these extreme values was not. This is more clearly shown in Fig. 1, which shows the range of LWC as a function of droplet MVD. The Federal Aviation Regulations Part 25 Appendix C certification envelope[22] is shown for comparison.

Table 1 Number of ice shapes for each airfoil

Airfoil	No. of conditions	No. of repeat runs	No. of off-centerline tracings	No. of duplicate tracings	Total
NACA 23014(mod)	40	22	8	0	70
LTHS	27	1	52	0	80
GLC 305	76	4	36	4	120
NACA 0012	57	125	305	3	490
NACA 4415(mod)	18	11	39	0	68
NLF 0414	8	0	0	0	8
NACA 0015	5	1	0	0	6
Totals	231	164	440	7	842

Table 2 Range of conditions in experimental database

Parameter	Range
Time	2–45 min
Chord	14–78 in.
Angle of attack	−4– +7 deg
Velocity	56–146 m/s
Reynolds number	2.3–13 × 10^6
Mach number	0.17–0.45
LWC	0.31–1.8 g/m^3
MVD	15–270 μm
Static temperature	−25.3–26.7°F
Total temperature	−15–33°F

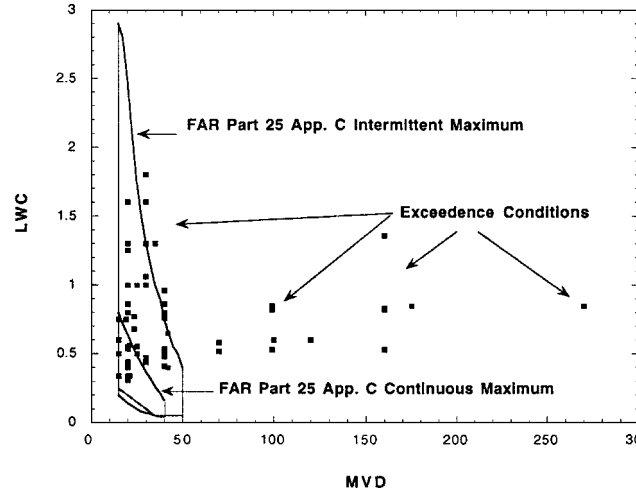

Fig. 1 Range of experimental data.

Figure 1 also shows that, although most of the conditions are within the certification envelopes, there are a number of cases in exceedence conditions. Note, however, that Fig. 1 is an incomplete description of the comparison of the certification envelope because temperature and exposure time also contribute to the definition of these curves.

The data are taken in the IRT by cutting out a small section of the ice growth and tracing the contour of the ice shape onto a cardboard template with a pencil. The pencil tracing is then transformed into digital coordinates with a hand-held digitizer. Recently, a flat-bed scanner with digitizing software has been available to accelerate the data acquisition process. For any given IRT test run, up to five spanwise sections of the ice shape are traced and digitized in this manner. There are several steps within this process that can potentially cause experimental error. Those that can be quantified by the current technique are the spanwise variability, the repeatability of an ice shape from one run to another, and errors involved in the tracing technique.

Spanwise Variability

Spanwise variability is the cross section to cross section variation of an ice accretion along the span of the test airfoil. Except for the NACA 23014(mod) model, all of the models used for this comparison are two-dimensional models. Because the spanwise variation for this model is very slight, it was also considered two-dimensional for comparison purposes. A two-dimensional model has a constant cross section in the spanwise direction and is mounted in the test section without any sweep angle. Even with a two dimensional model, the ice shape produced in the tunnel will have some spanwise variability due to the random nature of the ice accretion process. One means that has been used in the IRT to assess this variability is to take ice tracings at several spanwise sections. In the cited reports, the variability was assessed in the same qualitative manner as comparisons of predicted ice shapes. One technique often used was to visually inspect the ice shape and the cardboard tracings for similarity in the spanwise direction. The shapes may also be digitized at each tracing location and plotted to assess the variability.

This report applies the quantitative scale described in Sec. IV for assessing both LEWICE predictions and the variability of the test condition. In both cases, the reported difference will be the difference between a measurement on a given ice shape and the average of the experimental measurements for that condition.

Repeatability

Repeatability is the variation of an ice shape cross section from one tunnel run to another. Several tests in the IRT have assessed experimental error by running the same flow and spray conditions for the same airfoil multiple times. Cases processed for this validation effort have been repeated by the researcher by immediately running the same condition again, by running the same condition on a different night than the original test, and by running the same condition in a different test entry with the same model. In the past for each of these cases, the researcher would apply the same qualitative assessment of the repeatability of the condition. This study will apply the quantitative scale described in Sec. IV for assessing LEWICE predictions for assessing the quantitative repeatability of ice shapes in the IRT.

Tracing Technique

There are several potential errors involved in the ice tracing and digitization process that in the past have been difficult to quantify. Some of these errors are the quality of the template, the technique used by the researcher to trace the ice shape, and the digitization process.

The template is a rectangular piece of cardboard that has the contour of the airfoil cut into it. This is shown in Fig. 2. As can be seen from Fig. 2, if the ice shape extends beyond the dimensions of the template, it cannot be traced. Additionally, in the past the contour of the airfoil was not always cut precisely into the template so that the template may not have fit squarely onto the airfoil. More recent tracing techniques use registration marks to ensure precise fit.

The technique used by the researcher also may have an effect on the final digitized ice shape. The template may not be placed squarely on the airfoil or the researcher may only trace the tops of ice feathers or not trace feathers at all because the feather may break off due to the pressure applied by the pencil. The researcher may not always trace a single continuous line for the ice shape, making the digitization process more difficult. To assess these potential errors, researchers may trace the ice shape more than once or have more than one person trace the same shape. These tracings were then compared in the same qualitative manner as used for spanwise variability and repeatability.

Multiple tracings of the same ice shape are rarely performed in the IRT and even more rarely are both tracings digitized. Those that have been digitized are included in this report to provide a more quantitative assessment of the errors involved in the data acquisition process. It will be shown that despite the problems listed here, the quantitative errors due to tracing issues are minor in comparison to other sources of error.

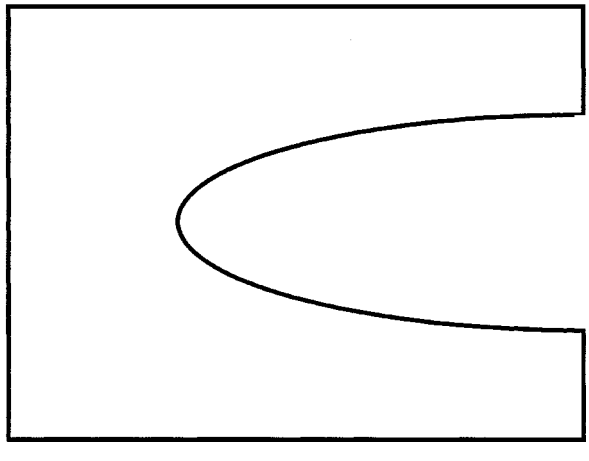

Fig. 2 Example of a cardboard template for tracing ice shapes.

IV. Description of Comparison Method

This section describes the methodology used to make the quantitative measurements on experimental and predicted ice shapes. This methodology has been incorporated into a computer code THICK, which calculates and outputs the parameters described. THICK was created to process the large number of ice shapes presented in this report. This program reads two geometry files: one for the clean airfoil and one containing an ice shape. This code will also be documented more thoroughly in the LEWICE 2.0 User Manual.[1] The following sections describe the calculations made by the THICK program.

Calculation of Ice Thickness

The ice thickness distribution for both experimental ice shapes and LEWICE ice shapes is determined by using a combination of two measurement techniques. The thickness is first measured by calculating the minimum distance from each point on the ice shape to a point on the clean surface. If the distribution of points on the clean surface is sufficiently concentrated, this procedure will provide a good approximation to the actual ice thickness. For this effort, each clean airfoil geometry contained over 5000 points to ensure the quality of the calculation.

The initial approach used for determining ice thickness used the unit normal from the surface. Even for a dense distribution of surface points, this method failed to determine ice thickness at every location on complex ice shapes. This is shown in Fig. 3. As seen in Fig. 3, the unit normal from the surface diverges outward. Even for a geometry with over 5000 surface points, a unit normal approach could not accurately capture details of the thickness distribution on the large and complex ice shapes analyzed for this paper. This was especially true of experimental ice shapes that have a large amount of detail.

The minimum distance approach will more accurately determine large ice thicknesses. This has been assessed via direct measurement of ice thicknesses with a ruler. For very small ice thicknesses, however, the accuracy is lessened as the thickness nears the resolution of the surface geometry. This is shown in Fig. 4.

The procedure used is to first calculate the thickness using the minimum distance approach. When this thickness becomes less than the segment length of either the iced or clean surface, it is then recalculated using the unit normal approach. Using the approach described, a unique ice thickness is determined for each point on the ice shape. At each point on the clean surface, however, it is possible to have regions where there is no recorded thickness or for a point to have more than one thickness value. This is shown in Fig. 5.

In the first case, where there is no thickness recorded, a thickness value at the clean surface can be interpolated from the values that have been obtained. In the second case, where more than one value exists, the maximum ice thickness value is recorded.

Determination of Icing Limits

The upper and lower limits of ice accretion for both experimental shapes and LEWICE shapes are easily found from the ice thickness distribution. They are located at the points on the clean airfoil where

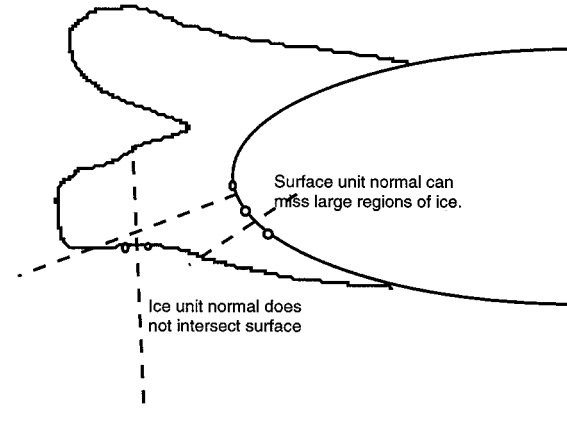

Fig. 3 Limitations of unit normal approach for ice thickness.

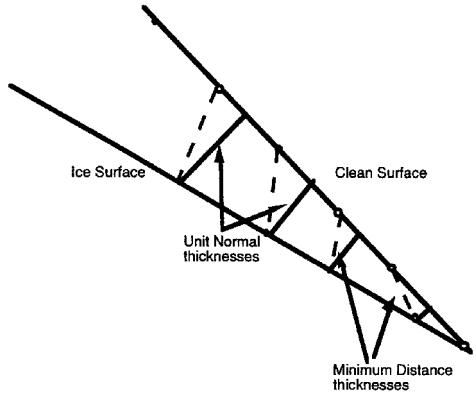

Fig. 4 Limitations of minimum distance approach.

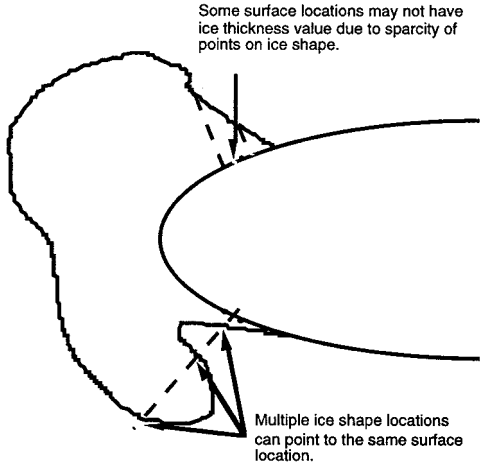

Fig. 5 Corrections to ice thickness distribution.

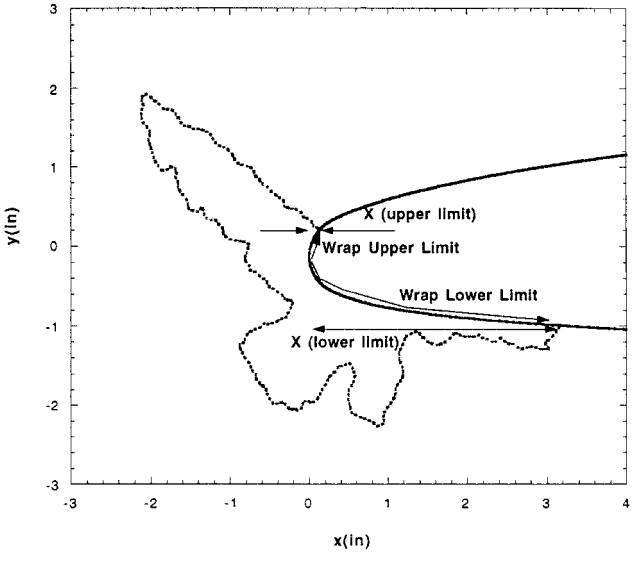

Fig. 6 Icing limits on sample ice shape.

the ice thickness first changes from zero as measured from the trailing edge. Experimental ice shapes may have sections where parts of the ice (ice feathers) are isolated from the main ice shape. This definition extends the icing limit to include this section of the ice shape. Also note that the definition used for icing limit is distinct from the impingement limit, which only refers to the extent of water collection on the airfoil. Both the surface distance from the leading edge and the x distance are recorded for each icing limit. The icing limits are shown in Fig. 6 on a sample ice shape. Figure 7 shows the icing limits on the ice thickness plot for this ice shape.

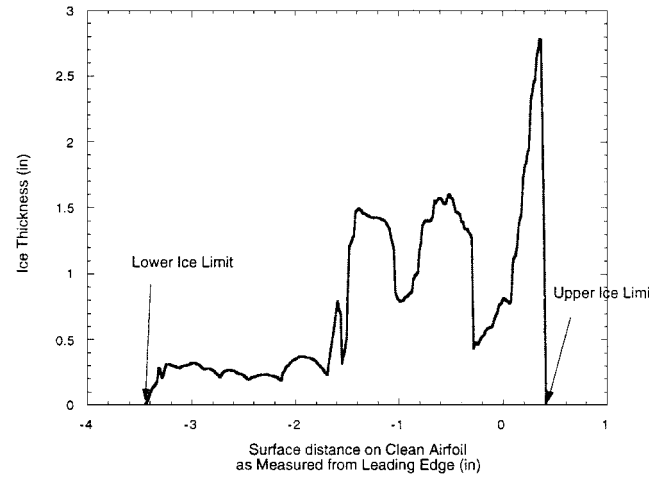

Fig. 7 Icing limits using ice thickness distribution.

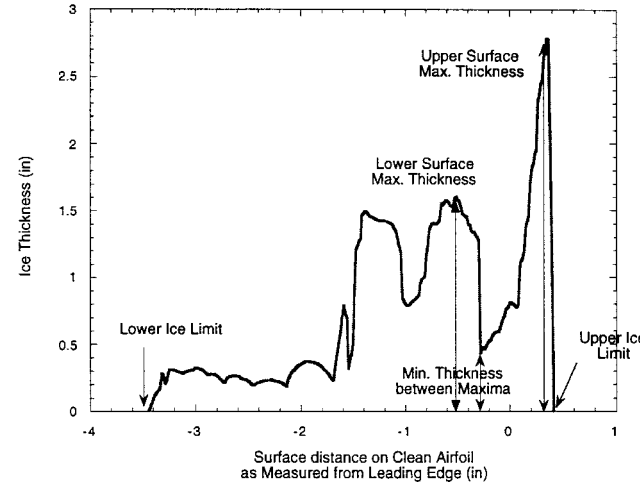

Fig. 8 Ice thickness values on sample ice shape.

Determination of Maximum and Minimum Thicknesses

Three ice thicknesses were selected for the quantitative analysis, the upper surface maximum thickness, the lower surface maximum, thickness, and the minimum thickness between these two maxima. These thicknesses are shown in Fig. 8. In Fig. 8, the upper surface and lower surface maxima clearly correspond to the classic definition of a glaze ice horn because the maximum ice thickness is quite large and extends far above the minimum thickness at the leading edge. For other conditions this may not be the case; hence, the term maximum thickness is used rather than horn thickness. This differentiation is usually found on smaller ice shape for which the maximum thickness is not easily seen. This is shown in Fig. 9.

For the upper surface and lower surface maximum thickness, the x and y locations at the maxima are also saved for calculation of a maximum thickness angle. The minimum thickness between the two maxima is also recorded. This thickness is often termed the stagnation point thickness, but the aerodynamic stagnation point is not necessarily at this location. In this report, the term minimum leading-edge thickness is used instead.

For a rime ice shape, the term horn does not apply, nor are there two distinct maxima to record. For this case, only the maximum ice thickness and the x and y locations at this maxima are recorded.

Determination of Maximum Thickness Angle

The maximum thickness alone does not adequately capture all of the necessary quantitative attributes desired. Some indication of where that maximum thickness occurred is also desirable. For this effort, the x and y locations at the maximum thickness were recorded for each ice shape, both experimental and for LEWICE. An angle at

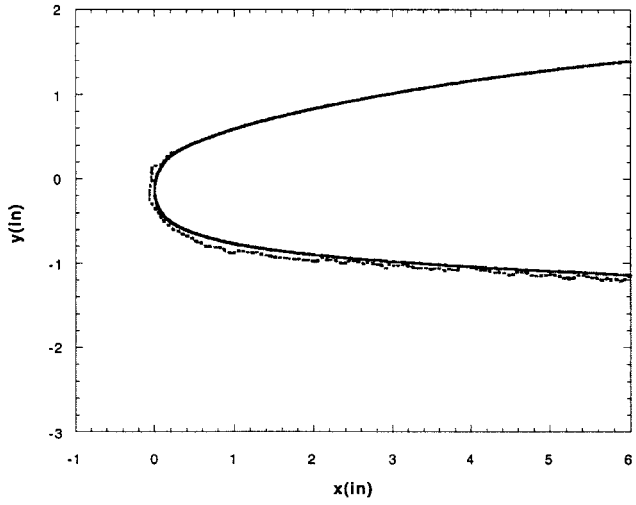

Fig. 9 Ice shape with peak thickness but no discernible horn.

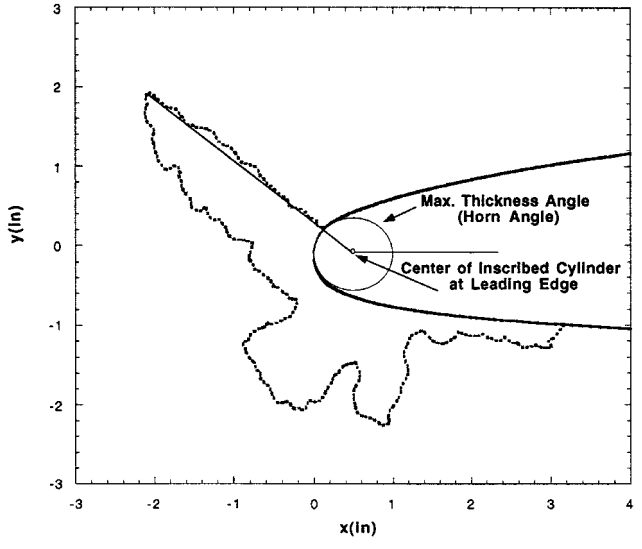

Fig. 10 Maximum thickness angle on sample ice shape.

the maximum thickness is then calculated. The reference location for all cases is the center of the inscribed circular cylinder at the leading edge for each airfoil. This is shown in Fig. 10.

Again note the terminology of maximum thickness angle. As discussed earlier, not all ice shapes have a classic glaze ice horn, but every ice shape has a maximum thickness. Where a glaze ice horn does exist, however, this measurement does define the horn angle.

Determination of Ice Area

The iced area calculated is not a true area. Because of time constraints, a more simplified calculation was performed by integrating the ice thickness calculated with respect to the surface distance, as given by

$$A = \int t\, ds \tag{1}$$

The approach used is valuable for quantitatively assessing ice shape features such as horn width, which are not included in the other parameters.

For the large number of points used on the clean surface, the calculation given is a reasonable approximation of area. Three areas are recorded: the total iced area, the lower surface area, and the upper surface area. The lower surface area is defined as the ice area below the leading edge (LE), and the upper surface ice area is calculated by subtracting the lower surface value from the total. For complex ice shapes, where the ice thickness is multiply defined as is shown in Fig. 5, this method for calculating ice area will result in an overstatement of the actual ice area.

V. Procedure for the LEWICE Runs

There are 231 cases run with LEWICE for this validation study. This is the complete set of unique conditions, inasmuch as 164 of the 395 test entries are repeat conditions. All of the cases run for this validation test were performed using the same procedure on a Silicon Graphics Indigo2 to ensure the consistency of the LEWICE predictions. It is well known that a user of an ice accretion code may alter the ice shape prediction by varying the time step and/or the panel spacing to improve the ice shape prediction. Users of early versions of LEWICE also altered the sand-grain roughness of ice to modify the prediction. These procedures were not followed for the validation runs. Sand-grain roughness has been a predicted value within LEWICE for several years. Additionally, for every run, the point spacing was fixed at a value of 4×10^{-4} (dimensionless). This was the smallest value that could be used for the array sizes in the program. The time step for all runs was 1 min for cases where the accretion time was 15 min or less. For longer runs, an automated procedure was implemented based on accumulation parameter, which is given by Eq. (2). When the accumulation parameter exceeded 0.01 for that time step, a new time step was started. The number of time steps is calculated internally in the program by Eq. (3). The equations are as follows:

$$A_c = \frac{(\text{LWC})(V)(\text{time})}{(\text{chord})(\rho_{\text{ice}})} \tag{2}$$

$$N = \frac{(\text{LWC})(V)(\text{time})}{(\text{chord})(\rho_{\text{ice}})(0.01)} \tag{3}$$

where

A_c = accumulation parameter, dimensionless
N = number of time steps, dimensionless
V = velocity, m/s
time = accretion time, s
chord = airfoil chord, m
ρ_{ice} = ice density, 9.17×10^5 g/m^3

and LWC is in grams per cubic meter.

The variability of LEWICE results for various time steps and point spacings is discussed in the section on Numerical Variability in the validation report.[2] The LEWICE cases had an additional correction due to the use of a potential flow code for the flow solution. As shown in Fig. 11, a potential flow code will overpredict lift coefficient especially at high angles of attack. To compensate for this, all LEWICE cases were run using a corrected angle of attack. This

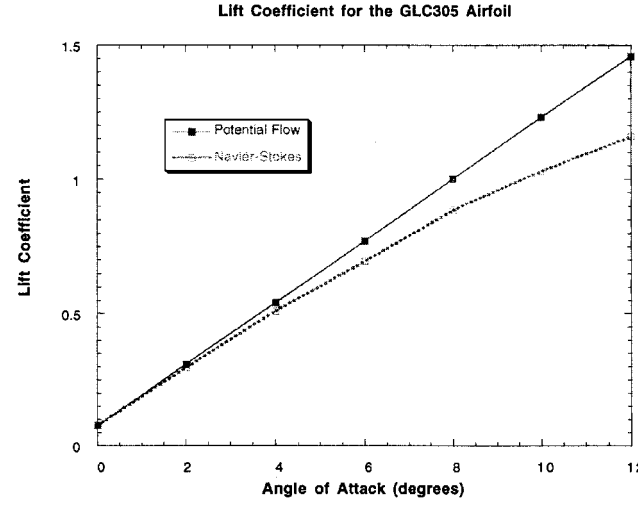

Fig. 11 Example of lift overprediction by potential flow.

is determined by equating the lift coefficient predicted by LEWICE on the clean airfoil for a given case with the lift coefficient on the airfoil at the angle of attack run in the tunnel.

VI. Quantitative Results

For each of the 842 experimental ice shapes and 231 predicted ice shapes, the quantitative measurements described earlier were taken and then entered into a Microsoft Excel® spreadsheet. A description of the exact contents of this spreadsheet is given in the validation report.[2] In Ref. 2, each of the 231 ice shapes is plotted against the tunnel centerline ice shape for that condition. The ice thickness distribution is also plotted. This paper will provide a summary of results of the quantitative comparison between the LEWICE predicted shape and the experimental average as well as the comparison of individual experimental ice shapes to this average. In each case, the experimental average for a given quantity is the average of all experimental ice shapes at that condition. Repeat runs and off-centerline measurements are averaged with the centerline value to arrive at this measurement. Table 3 provides the average variation for LEWICE and each experimental error. The uncertainties shown in Table 3 show the standard deviation of the values, which were only calculated for the overall experimental error and for the LEWICE predictions. Table 4 provides the median values for each measurement, in terms of both the median of the absolute differences (for both LEWICE and the experimental data) and the median of the original differences for the LEWICE results. This last was provided to show that the LEWICE predictions lay on both sides of the experimental average; i.e., that generalities that state that LEWICE always or usually overpredicts or underpredicts a specific parameter are not reflected in these data.

An example calculation has been included from the icing limit calculation for run 251 in the NACA 23014(mod) database. This case was chosen arbitrarily inasmuch as no single case can truly be considered representative of the entire database. For this case, there was a single IRT run at that condition and three tracings were taken at the 30-in. span, 36-in. span (midspan location) and 42-in. span. For the example case, the measured lower surface icing limits were 12.85, 12.66, and 11.36 in. from the LE at the 30-, 36-, and 42-in. span locations, respectively. The experimental average is 12.29 in. The predicted lower icing limit was 13.4 in. from the LE. The chord for this airfoil was 68.7 in. Therefore, the spanwise variability (in this case the overall variability as well inasmuch as no other data exist) for the three tracings are 0.81, 0.53, and −1.35% of chord with an absolute average of 0.9% chord. The LEWICE prediction for this case is 1.6% chord from the experimental average.

Icing Limits

The icing limits are the chordwise locations on the ice shape on the upper and lower surface where the ice shape merges with the airfoil. Both the surface distance from the LE and the x distance are recorded for each icing limit. The results presented are for the surface distance values.

The first two rows of Table 3 show the results of all icing limit measurements for both the experimental ice shapes and for LEWICE. These results are presented as a percentage of chord to normalize the results for different cases. Table 3 shows that the average of the experimental variations in the lower icing limit is 2% of chord whereas the LEWICE values lie within 6% of chord from the experimental average value on average. This result uses the absolute error for each case to compute the average variation. Contrary to popular belief, in the majority of cases LEWICE underpredicts rather than overpredicts the icing limit as compared to the experimental data, as shown in Table 4. This result can likely be attributed to the use of a monodispersed drop size distribution when obtaining the predicted result.

Maximum Ice Thickness (Horns)

The details of the ice thickness calculation were presented in Sec. IV. As discussed in Sec. IV, the measurement of a maximum thickness is not necessarily the thickness of a glaze ice horn. Where the ice shape does have a glaze ice horn, the maximum thickness does give the horn thickness. To compare different conditions with different chord lengths and accretion conditions, the individual ice thicknesses were nondimensionalized by the maximum accumulation thickness as

$$t_{\max} = \frac{(\mathrm{LWC})(V)(\mathrm{time})}{\rho_{\mathrm{ice}}} \tag{4}$$

This factor is, on average, twice as much as the maximum upper surface thickness. Rows 3–5 in Table 3 show the dimensionless difference in ice thickness for the three ice thickness measurements made in this report. Results are presented for the variation of tunnel repeatability, spanwise variability, tracing error as well as for the overall experimental error and for LEWICE. This table shows that the maximum thicknesses can be measured to within 5% experimentally and that the average difference for the LEWICE cases is 11% for maximum thickness.

Table 4 Median values for LEWICE differences and experimental errors

Measurement	LEWICE median (signed)	LEWICE medial (absolute)	Experimental median (absolute)
Lower icing limit	−2.56	3.16	1.02
Upper icing limit	0.33	0.81	0.31
Lower maximum thickness	7.98	9.71	3.17
LE minimum thickness	1.48	5.16	1.66
Upper maximum thickness	−2.45	9.35	4.16
Lower surface area	2.63	4.54	1.8
Upper surface area	−1.26	2.05	0.62
Total area	1.32	5.74	2.23
Lower horn angle	1.2	17.84	5.71
Upper horn angle	9.52	14.67	3.29
Angle difference	−8.16	21.61	8.75
Overall	0.91	5.07	1.88

Table 3 Average variation of experimental data and average LEWICE comparison to average experimental values

Measurement	LEWICE	Repeatability	Spanwise variability	Tracing technique	Experimental error
Lower icing limit	6.11 ± 5.17	1.44	1.89	0.60	1.62 ± 1.72
Upper icing limit	1.64 ± 6.94	0.51	0.52	0.82	0.52 ± 0.631
Lower maximum thickness	11.72 ± 7.91	3.90	4.03	1.79	3.90 ± 3.51
LE minimum thickness	5.74 ± 4.76	2.63	2.15	0.57	2.37 ± 3.04
Upper maximum thickness	9.78 ± 8.60	4.29	5.34	3.69	4.74 ± 4.48
Lower surface area	8.46 ± 8.99	2.96	2.69	0.97	2.80 ± 3.00
Upper surface area	4.13 ± 2.88	0.78	0.89	0.76	0.83 ± 0.822
Total area	9.91 ± 9.27	3.44	3.21	1.01	3.29 ± 3.39
Lower horn angle	29.63 ± 20.77	9.13	10.66	1.06	9.57 ± 15.69
Upper horn angle	16.58 ± 12.77	5.69	5.98	3.37	5.77 ± 7.23
Angle difference	33.51 ± 25.14	12.47	14.40	4.04	13.07 ± 17.1
Overall	7.20 ± 3.88	2.50	2.60	1.30	2.50 ± 1.76

Ice Area

The comparison of ice area for the different cases also poses a problem. A fair comparison across the varied conditions and airfoil sizes is difficult. In this report, the area difference has been nondimensionalized by the maximum accumulation thickness given earlier and by the airfoil thickness as

$$\text{area}_{\text{nondimensionalized}} = \frac{\text{area}_{\text{measured}}}{(t_{\max})(\text{thickness}_{\text{airfoil}})} \tag{5}$$

Conceptually, this nondimensionalizes the area by a length scale ($t_{\max}$) and a width scale (airfoil thickness). It should be noted that the absolute values for ice area are maintained in the Excel spreadsheet so that the users of these data can make their own comparisons.

Rows 6–8 of Table 3 show the results for the ice area comparison. Values for the upper surface ice area, lower surface ice area, and overall ice area are shown for each of the categories described earlier. This table shows that the experimental difference in ice area is less than 4% on the scale given whereas for the LEWICE results the variation is approximately 10%.

Angle at Maximum Thickness (Horn Angle)

As described earlier, the horn angle was measured with respect to a horizontal line that goes through the center of the inscribed cylinder at the LE. This angle was measured for all ice shapes whether or not they fit the classical definition of having a glaze ice horn. Many experimental ice shapes were in the form of distributed roughness with several peaks, which can cause a large amount of scatter in the experimental results shown.

Rows 9–11 of Table 3 show the variation in maximum thickness angle for LEWICE and for the experimental categories described earlier. Results are presented in degrees. This figure shows that the variation in the experimental data is 6 deg for the upper angle, 10 deg for the lower angle, and 13 deg for the difference between these angles. The LEWICE difference from the experimental average are 16 deg for the upper angle, 30 deg for the lower angle and 33 deg for the angle difference.

Overall Assessment

Once the individual measurements are taken for each ice shape, it becomes useful to create an overall assessment of the ice shape prediction. Because each measurement is different, several methods could be used to assess the overall difference between two ice shapes. In this paper, 8 of the 11 measured values presented have been nondimensionalized. Angles do not have a characteristic measure to use for nondimensionalization, and so the three angle criteria are reported in degrees. Because not all of the measured quantities can be nondimensionalized, two overall assessment factors have been calculated. The first overall assessment was determined by an average of the eight individual dimensionless values and the three angle criteria in degrees. The second overall assessment was calculated by using only the eight dimensionless measurements.

Figure 12 show the comparison of the first overall assessment for each of the experimental errors and for LEWICE. This calculation shows an average overall difference of approximately 4.4 for the experimental database and 12.5 for LEWICE. Because the angle criteria are not dimensionless, these numbers cannot be considered a percent difference. The last row of Table 3 and Fig. 13 shows the comparison using the second overall assessment. This second calculation shows an average overall difference of 2.5% for the experimental data and 7.2% for LEWICE. The standard deviation is 1.8% for the experimental data and 4% for the LEWICE results. To determine if this simple average is a good assessment of the variation, plots were made of the average variation for the experimental shapes and for the LEWICE shapes.

Figure 14 shows an example of two ice shapes that are near the overall experimental average. Figure 14 shows the spanwise variability from a data point in the NACA 4415(mod) database. The qualitative comparison of these two ice shapes suggests that the overall assessment parameter is a reasonable approximation. Figure 15 shows an example of two ice shapes that are near the experimental average plus one standard deviation. According to the method described, these ice shapes are more dissimilar than the ice shapes in Fig. 14. This is difficult to assess from Fig. 15 inasmuch as the ice shape therein is quite small. Other ice shapes that have a similar percent difference are likewise quite small. Conceptually this makes sense, as the same absolute difference in any measurement will result in a larger percentage difference on a smaller ice shape.

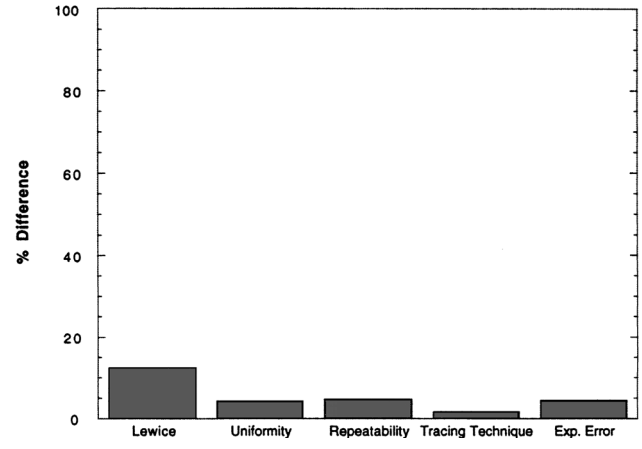

Fig. 12 Overall ice shape variation compared to average experimental value.

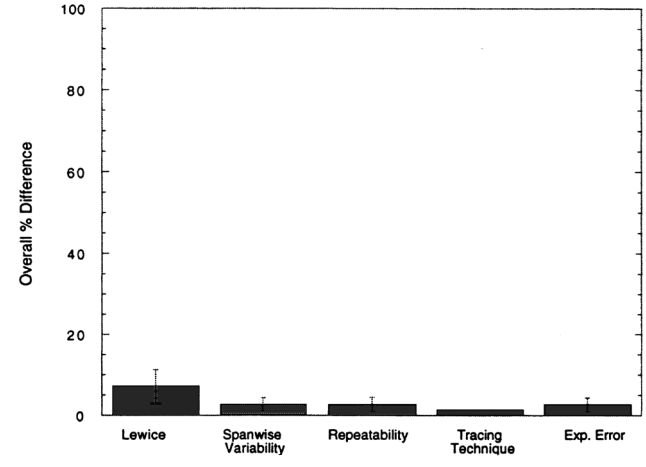

Fig. 13 Overall percentage difference from average experimental measurements.

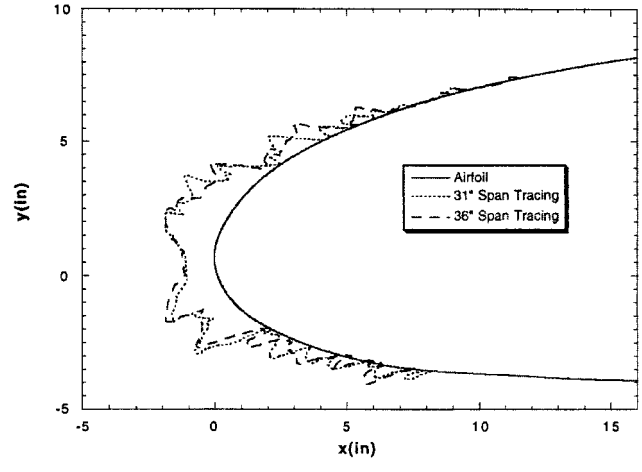

Fig. 14 Example of ice shape variation at average % difference in experimental data.

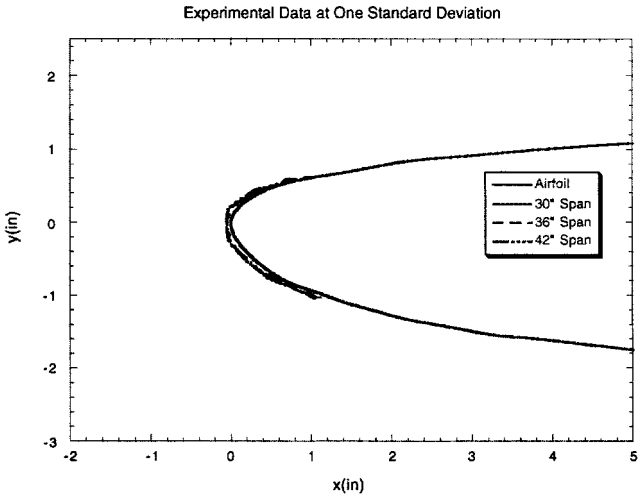

Fig. 15 Example of ice shape variation at one standard deviation above average % difference.

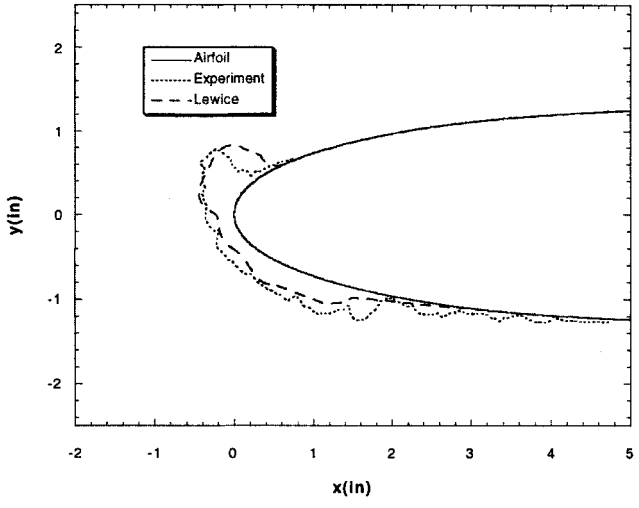

Fig. 16 Example of ice shape prediction at average % difference in experimental data.

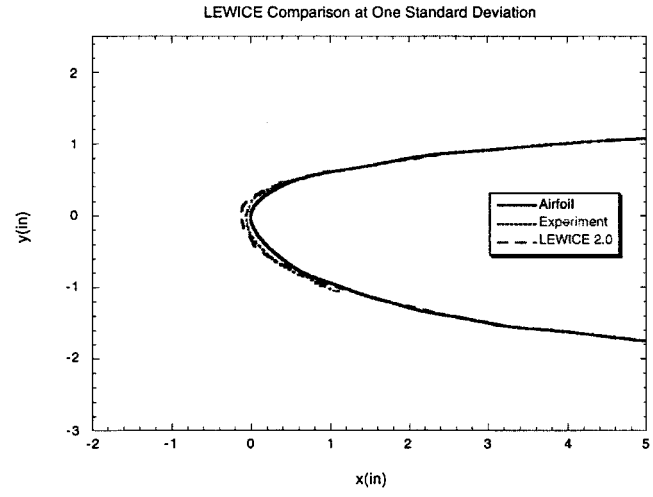

Fig. 17 Example of ice shape prediction at one standard deviation above average % difference.

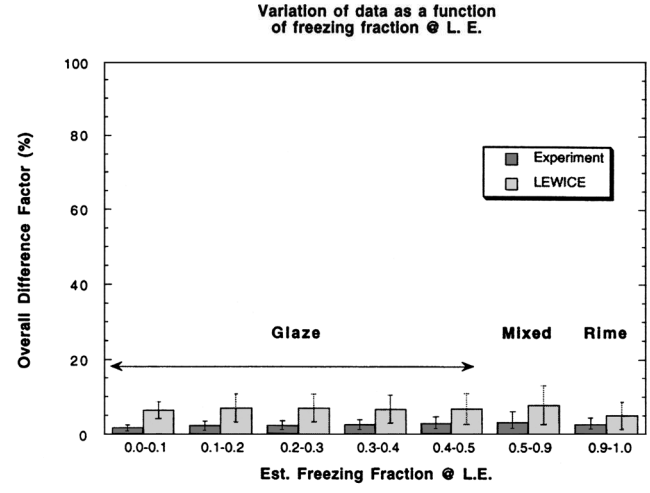

Fig. 18 Variation of results as a function of ice type.

Similarly, Fig. 16 shows an example that is at the average variation for the LEWICE cases, whereas Fig. 17 shows an example at one standard deviation above the average. The qualitative assessment of these comparisons also agrees with the overall assessment parameter used.

One use for the quantitative measurements that have been obtained would be to determine if any trends existed in the database. For instance, it may be possible at some point to determine if the LEWICE predictions are better for certain airfoils or certain icing conditions or if certain tests produced better data than other tests. Unfortunately, even though the database is quite large when used collectively, there are insufficient data in many cases to produce any conclusions. For example, Table 1 shows that there are 164 repeat runs in the database. However, 76% of these data are exclusive to one airfoil, the NACA 0012. At most, only one other airfoil (NACA 23014) has sufficient data to assess repeatability independently. Similar restraints can be seen for other factors.

One possible trend can be seen in Fig. 18, which shows the overall variability of the experimental data and the LEWICE difference from the experimental average as a function of the estimated freezing fraction at the LE. This factor was calculated from

$$\text{freezing fraction} = \frac{\text{minimum thickness at LE}}{\text{maximum ice thickness}} \qquad (6)$$

and can only be considered an approximate calculation. The actual freezing fraction cannot be calculated from the experimental ice shapes. This factor, however, will show the general trend. At low values, the maximum ice thickness is large compared to the LE thickness, which is indicative of a glaze ice shape. At higher values, there is no pronounced ice horn, which is indicative of rime ice shapes. Additionally, the factor is bounded in the region $0 \leq$ freezing fraction ≤ 1. Data in the 0.5–0.9 range were grouped inasmuch as there were insufficient data in each 0.1 range to consider those ranges statistically valid. The only trend that can be seen in this figure is that there is no trend. Each group of data lies within the error bars. It is possible to conclude from this figure that both the experimental data and LEWICE have a similar accuracy for glaze ice shapes as for rime ice shapes, a result that runs counter to conventional beliefs.

Improvements to Methodology

The technique used in this report for quantitative comparison of ice shapes represents only one possible path for quantitative validation of code results. Ruff and Anderson[23] proposed an alternate methodology for creating an overall assessment of ice shape prediction. Other methods can also be tested for creating an overall assessment of ice shape prediction. Because the number of cases in this database, an important consideration is the efficiency at which quantitative measurements can be taken and entered into a spreadsheet for analysis. The current technique used a stand-alone utility program written by the author to generate the ice thickness distributions. This code was very useful in generating the data needed for this comparison, but the process of transferring the information to the spreadsheet was time consuming. More efficient methods for acquiring the quantitative parameters will be developed in the future.

The definition of maximum thickness angle used in this report is not the only possible definition. Other definitions could use the chord line of the airfoil instead of a horizontal line. The reference point could be selected as the LE of the airfoil or the point on the clean surface where the ice thickness was defined. Because of time constraints, the definition presented was the only one calculated from the ice shapes.

It was stated in the Introduction that a quantitative analysis is only one facet of the code validation process. Once the comparison of ice shape has been made, it would be useful to quantify the difference in aeroperformance, i.e., lift, drag, moment coefficients, etc., based on the quantitative difference in geometry. This process would be very time consuming to perform on the entire database even at the fast processor speeds available now. A comparison of a selected number of these cases is being planned at this time. This comparison would calculate the difference in predicted aeroperformance for a given difference in ice shape, using both experimental ice shapes and predicted ice shapes from LEWICE. For example, this comparison would try to determine if the difference in aeroperformance for two ice shapes that are 10% different is consistently greater than the difference in aeroperformance for two ice shapes that are only 5% different.

VII. Conclusions

This paper has presented the quantitative comparisons of several geometric characteristics for a database of over 1000 ice shapes. Measurements of icing limit, ice thickness, ice area, and horn angle were made for each ice shape. Comparisons were made for the difference in experimental variations, such as tunnel repeatability, spanwise variability, and tracing errors. Comparisons were also made for the difference between the predicted ice shape from LEWICE and the average experimental value. Comparisons were made for each individual quantitative criterion. An overall assessment was made for the quantitative comparison as well.

This comparison shows that based on the overall assessment criteria presented, the variation in the experimental data was $2.5 \pm 1.8\%$ and the LEWICE predicted ice shape differs from the experimental average by $7.2 \pm 4\%$. The variation due to tracing technique was found to be statistically insignificant. The spanwise and repeat variability were found to be extremely close and at the same low level (2.5%). This may indicate that the variation in ice shape for either measure is a reflection of the chaotic nature of the icing phenomena and is not due to the tunnel dynamics. The accuracy of LEWICE predictions was shown to be statistically independent of ice type, i.e., the differences for glaze ice shapes and rime ice shapes showed similar accuracy as compared to the data. The ice shape data and output files from LEWICE that were generated for this paper are included on CD-ROMs along with all of the quantitative comparison numbers in a published contractor report.[2]

Acknowledgments

The author would like to thank the NASA Lewis Icing Branch for their continued support of this research, both financial and for their help with this paper. Special recognition goes to the researchers who generated the experimental data specifically, G. Addy, D. Anderson, S. Chen and T. Langhals, and C. S. Bidwell and J. F. VanZante, to Mark Potapczuk for his insights, and especially to Tammy Langhals for digitizing all of the experimental ice tracings.

References

[1]Wright, W. B., "Users Manual for the NASA Lewis Ice Accretion Code LEWICE 2.0," NASA CR 208690, Feb. 1999.

[2]Wright, W. B., and Rutkowski, A., "Validation Results for LEWICE 2.0," NASA CR 208690, Jan. 1999.

[3]Wright, W. B., Gent, R. W., and Guffond, D., "DRA/NASA/ONERA Collaboration on Icing Research Part II—Prediction of Airfoil Ice Accretion," NASA CR 202349, May 1997.

[4]Gent, R. W., "TRAJICE2—A Combined Water Droplet and Ice Accretion Prediction Codes for Airfoils," Royal Aircraft Establishment, RAE TR 90054, Nov. 1990.

[5]Hedde, T., and Guffond, D., "Improvement of the ONERA 3-D Icing Code, Comparison with 3D Experimental Shapes," AIAA Paper 93-0169, Jan. 1993.

[6]Brahimi, M. T., Tran, P., and Paraschivoiu, I., "Numerical Simulation and Thermodynamic Analysis of Ice Accretion on Aircraft Wings," Centre de Développement Technologique de l'École Ploytechnique de Montreal, CDT Project C159, Final Rept., Montreal, PQ, Canada, May 1994.

[7]Tran, P., Brahimi, M. T., Tezok, F., and Paraschivoiu, I., "Numerical Simulation of Ice Accretion on Multi-Element Configurations," AIAA Paper 96-0869, Jan. 1996.

[8]Mingione, G., Brandi, V., and Esposito, B., "Ice Accretion Prediction on Multi-Element Airfoils," AIAA Paper 97-0177, Jan. 1997.

[9]Olsen, W., Shaw, R., and Newton, J., "Ice Shapes and the Resulting Drag Increase for a NACA 0012 Airfoil," NASA TM-83556, Jan. 1983.

[10]Addy, G. E., Potapczuk, M. G., and Sheldon, D., "Modern Airfoil Ice Accretions," AIAA Paper 97-0174, Jan. 1997.

[11]Wright, W. B., and Potapczuk, M. G., "Comparison of LEWICE 1.6 and LEWICE/NS with IRT Experimental Data from Modern Airfoil Tests," AIAA Paper 97-0175, Jan. 1997.

[12]Wright, W. B., and Bidwell, C. S., "Additional Improvements to the NASA Lewis Ice Accretion Code LEWICE," AIAA Paper 95-0752, Jan. 1995.

[13]Wright, W. B., "Users Manual for the Improved NASA Lewis Ice Accretion Code LEWICE 1.6," NASA CR 198355, June 1995.

[14]Wright, W. B., Bidwell, C. S., Potapczuk, M. G., and Britton, R. K., *Proceedings of the LEWICE Workshop*, NASA, June 1995.

[15]Wright, W. B., "Capabilities of LEWICE 1.6 and Comparison with Experimental Data," *Proceedings of the SAE/AHS International Icing Symposium*, Society of Automotive Engineers/American Helicopter Society, Alexandria, VA, Sept. 1995, pp. 347–361.

[16]Wright, W. B., and Potapczuk, M. G., "Computational Simulation of Large Droplet Icing," Federal Aviation Administration, FAA Phase III Meeting, DOT/FAA/AR-96/81, II, May 1996.

[17]Shin, J., and Bond, T. H., "Results of an Icing Test on a NACA0012 Airfoil in the NASA Lewis Icing Research Tunnel," AIAA Paper 92-0647, Jan. 1992.

[18]Addy, H. E., Jr., Potapczuk, M. G., and Sheldon, D. W., "Modern Airfoil Ice Accretions," AIAA Paper 97-0174, Jan. 1997.

[19]Addy, H. E., Jr., Miller, D. R., and Ide, R. F., "A Study of Large Droplet Ice Accretion in the NASA Lewis IRT at Near-Freezing Conditions; Part 2," NASA TM 107424, May 1996.

[20]Miller, D. R., Addy, H. E., Jr., and Ide, R. F., "A Study of Large Droplet Ice Accretion in the NASA Lewis IRT at Near-Freezing Conditions," NASA TM 107142, Jan. 1996.

[21]Reehorst, A., Chung, J., Potapczuk, M., and Choo, Y., "The Operational Significance of an Experimental and Numerical Study of Icing Effects on Performance and Controllability," AIAA Paper 99-0374, Jan. 1999.

[22]"Airworthiness Standards: Transport Category Airplanes," Federal Aviation Regulations, FAR Pt. 25, U.S. Dept. of Transportation, Federal Aviation Administration, Washington, DC, March 1986.

[23]Ruff, G. A., and Anderson, D. N., "Quantification of Ice Accretions for Icing Scaling Evaluations," AIAA Paper 98-0195, Jan. 1998.